

# Brain Oscillatory and Network Activity during resting states

Sergio Ballesteros<sup>1</sup>, Olga Lazareva<sup>2</sup>

## Abstract

We analyzed the electroencephalography signals from a single subject with eyes-open and eyes-closed baseline conditions. We found significant differences at the frequency of alpha waves at 10 Hz. We studied the connectivity of the brain at that frequency using two MVAR estimators and found different variations in network topologies for both conditions and estimators. Also, we analyzed the presence of over-represented motifs in both topologies and filtered some patterns that are characteristic only for a certain condition. Finally, we did a topology study and in the occipital part of the brain we found differentiation in communities structures.

## Keywords

EEG — oscillation — network — motif — connectivity — community

<sup>1</sup>sergio@ballesteros.me

<sup>2</sup>olazareva1993@gmail.com

## Introduction

Electroencephalography (EEG) was invented in 1924 by German scientist Hans Berger and since then scientific interest to explain various human behavior and infer functional aspects of both normal and pathological brain processes with EEG was strongly increasing[1].

Not only different human behavior such as eye movement, attention and hand clenching can be visualized with EEG signals, but also human conditions such as schizophrenia [2] or intelligence [3]. All these states are associated with a particular frequency/frequencies that help us understand the functional behavior of complex brain structures. In this way, EEG allows us to acquire brain signals corresponding to various states.

In this work, we have concentrated on determining differences in two particular states: eyes open (O) and eyes closed (C). These differences are important to recognize when evaluating EEG research and should be considered when choosing eyes-open or eyes-closed baseline conditions for different research proposes. We have studied 64-channels EEG signals, corresponding to a single subject (N=1). Then we performed spectral, connectivity, graph indices, motifs and community detection analysis.

At each stage, we emphasized arising differences between C and O and then concluded the main identifiers of each state.

## 1. Methods

We downloaded the two *EDF+* files from [5] corresponding to two 64-channels EEG signals from a single subject<sup>1</sup>. One signal was obtained with the subject at rest with C, and the

other signal also at rest with O. The two signals on one channel can be observed in Figure 1.

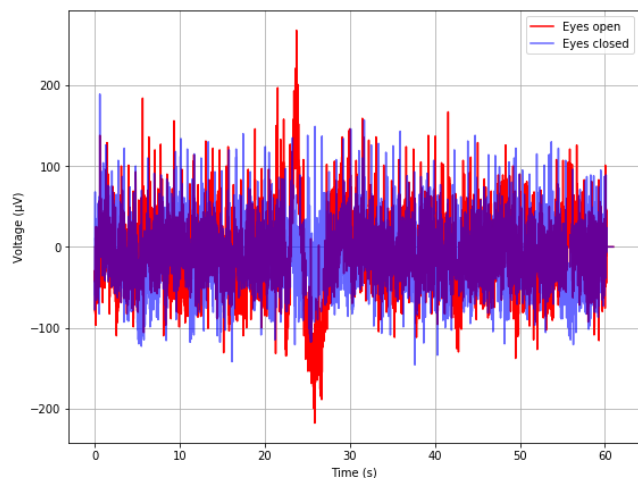


Figure 1. EEG of the channel Iz.

### 1.1 Spectral analysis

For the signal processing part we used the the python library *scipy.signal* [6]. We used the Welch method and Periodogram method, both implemented in the library, for computing the power spectral density (PSD) on all channels. As parameters we used a Hanning window and sampling frequency<sup>2</sup> of 160. In order to check statistically significant differences (SSD) on the PSDs of the states O and C, we conducted the Wilcoxon signed-rank test on each channel for the whole spectrum.

<sup>1</sup>The subject is denoted as S040 in the nomenclature used by [5]

<sup>2</sup>From [5] we know that the EEG signals were sampled at 160 samples per second

We chose this test because it is a non-parametric statistical hypothesis test that can be used when the samples are matched and the data is not normally distributed [7].

Also, we verified the differences in magnitude of C with respect to O, on each channel, using the Welch PSD for the whole spectrum and at 10 Hz, which corresponds to the peak of alpha waves. We used the accumulative normalized logarithmic differences (ANLD), which is defined as follows in the discrete domain for channel  $i$ :

$$ANLD_i = \frac{1}{ANLD_{max}} \sum_{f=0}^F |\log_{10}[PSD_O(f)] - \log_{10}[PSD_C(f)]| \quad (1)$$

Where  $F$  is the maximum frequency,  $PSD_O(f)$  is the PSD calculated at frequency  $f$  with state O and  $PSD_C(f)$  is with state C.

Finally, we studied the distributions of Welch PSD on O and C on all the channels together specifically in for the following brain waves: alpha (7.5 - 12.5 Hz), delta (1.5 - 3.5 Hz), theta (4 - 7 Hz) and beta (13.5 - 25 Hz). For alpha and beta, we used independent  $T$  - test given that we found that the distributions were normal, and for theta and delta we used the Mann-Whitney U test because their distributions were not normal.

## 1.2 Connectivity graph

In order to estimate graph connectivity two techniques were adopted: Partial Directed Coherence (PDC) and Directed Transfer Function (DFT).

PDC was calculated in the following way:

$$\pi_{i,j}(f) = \frac{|A_{i,j}(f)|^2}{\sum_{m=1}^L |A_{m,i}(f)|^2} \quad (2)$$

Where  $A_{i,j}(f)$  is i-th, j-th element of an autocorrelation matrix on a certain frequency.  $A_{i,j}(f)$  was calculated by fitting Multivariate Autoregressive Model of a format:

$$\begin{cases} x_1[n] = -\sum_{k=1}^p a_{1,1}[k]x_1[n-k] - \dots - \sum_{k=1}^p a_{1,N}[k]x_N[n-k] + e_1[n] \\ x_2[n] = -\sum_{k=1}^p a_{2,1}[k]x_1[n-k] - \dots - \sum_{k=1}^p a_{2,N}[k]x_N[n-k] + e_2[n] \\ \dots \\ x_N[n] = -\sum_{k=1}^p a_{N,1}[k]x_1[n-k] - \dots - \sum_{k=1}^p a_{N,N}[k]x_N[n-k] + e_N[n] \end{cases} \quad (3)$$

Where  $p$  is the order of the model which can be estimated with different model selection techniques like Akaike information criteria or Bayesian information criterion (BIC). In our work we used BIC as described bellow:

$$BIC = \ln(n)k - 2\ln(\hat{L}) \quad (4)$$

where  $n$  is the sample size,  $\hat{L}$  the maximized value of the likelihood function of the model,  $k$  is the number of parameters estimated by the model. For instance, as it shown in the Figure 2, estimation of the order of the MVAR model for C with BIC showed, that the optimal order is equal to two.

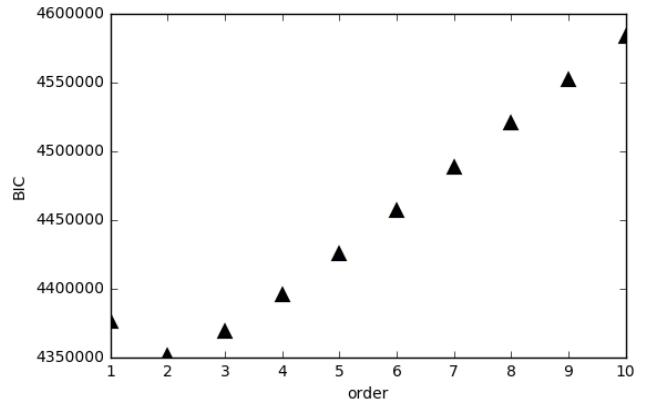


Figure 2. Order estimation with BIC for C

DTF was calculated in the following way:

$$v_{i,j}(f) = \frac{|H_{i,j}(f)|^2}{\sum_{m=1}^L |H_{m,i}(f)|^2} \quad (5)$$

Where  $H$  stands for the Hermitian transpose:

$$\begin{vmatrix} H_{1,1}(f), H_{1,2}(f), \dots, H_{1,N}(f) \\ H_{2,1}(f), H_{2,2}(f), \dots, H_{2,N}(f) \\ \dots \\ H_{N,1}(f), H_{N,2}(f), \dots, H_{N,N}(f) \end{vmatrix}$$

which is a matrix of suitable filters (fast Furrier transform in our case) described in the frequency domain.

The main difference between two MVAR estimators is that PDC aims to reconstruct patterns accurately, taking into account only direct influence, while DTF is also considering indirect effect.

For this analysis, we used the python tools provided by [4].

## 1.3 Graph theory indices

Using *networkx* we studied the structure of the PDC and DFT networks from a macroscopic point of view using two global indices: average clustering coefficient and average shortest path length and from a microscopical point of view using local indices we measured the total degree, in-degree and out-degree of each node.

The average clustering coefficient is defined as  $C = \frac{1}{n} \sum_{i=1}^n C_i$  where  $n$  is the number of all vertices and where

$$C_i = \frac{|\{e_{jk} : v_j, v_k \in N_i, e_{jk} \in E\}|}{k_i(k_i - 1)} \quad (6)$$

Also  $k_i$  is the number of neighbours of a vertex,  $e_{ij}$  is the edge that connect  $v_i$  with  $v_j$ ,  $N_i$  is the neighbourhood of  $v_i$  and  $E$  is the set of all edges.

The average shortest paths length is defined as

$$l_g = \frac{\sum_{i=1, i \neq j}^n d(v_i, v_j)}{n(n-1)} \quad (7)$$

Where  $d(v_i, v_j)$  denotes the shortest distance between vertices  $i$  and  $j$ .

#### 1.4 Motif analysis

In this work, we have focused on a search for all possible 3 and 4 nodes motifs in a network.

Firstly, we have developed an algorithm which is able to return all possible n-nodes motifs. The main intuition was: 1) to make a list of all possible edges between two nodes 2) consider all possible combinations of those pairs on length  $(n - 1)$  which include all n-nodes 3) repeat point 3 for a length equal to  $n$ ,  $n+1$  and so on up to the point there will not be a chance to build a configuration with unique edges 4) convert each configuration to a directed graph and save it only if it is isomorphic to all graphs that were built before.

Thus, we have 13 motifs for 3-nodes configuration and 201 motifs for 4-nodes configuration.

In order to count all given motifs in a network, we divided the network into all possible n nodes sub-graphs and then we checked, each of them if they are isomorphic to one of the motifs. In this way, we got all structural motifs.

We chose this deterministic approach since the size of the network and amount of motifs allows us to perform the computations in the most accurate way, otherwise, with a bigger network, we would go with some of the approximation methods.

In order to determine over-represented motifs and anti-motifs we performed the following tests:

$$P(f_{\text{random}}(G_k) - f_{\text{original}}(G_k) < P) \quad (8)$$

$$P(f_{\text{random}}(G_k) - f_{\text{original}}(G_k) > D * f_{\text{random}}(G_k)) \quad (9)$$

Where  $G_k$  is a motif of a graph  $G$ ,  $f_{\text{random}}(G_k)$  is a frequency of a certain motif in a random network,  $f_{\text{original}}(G_k)$  is a frequency of a certain motif in the original network,  $P$  was set to 0.05 and  $D$  to 0.5. In this way, we say that a motif  $G_k$  is over-represented with 95% probability if (6) is true. Also, a motif  $G_k$  may be an anti-motif if in a random network it appears more than twice more often then in the original network.

To perform those tests we had to generate random networks. To do this we used an algorithm from Milo et al [11]. The goal was to create a randomized connectivity matrix  $M_{\text{rand}}$ , which has the same number of nonzero elements in each row and column as the corresponding row and column of the real connectivity matrix.

#### 1.5 Community detection

To detect communities we used the Louvain algorithm which is modularity based and it was performed in two steps. First, it iterates through all the nodes in the network and assigns each node to a community as long as it increases the modularity. Afterwards, supernodes are created from the clusters of the

first step and the process is repeated again until convergence [8].

Unfortunately this algorithm is not implemented for directed networks on *networkx*, so we used instead the *igraph* python library, where it is implemented [9].

## 2. Results and Discussion

### 2.1 Spectral analysis

Both the Welch method as well as the Periodogram method showed that on all channels it exists a peak at around 10 Hz when the subject had the eyes closed but not when the eyes were open. This behavior happened on most of the channels, and we show it for channel Iz on Figures 3 and 4. Moreover, there are two other peaks at around 2 Hz and at 60 Hz which appear on both O and C. Other PSDs Figures of other relevant channels can be found in Appendix A.

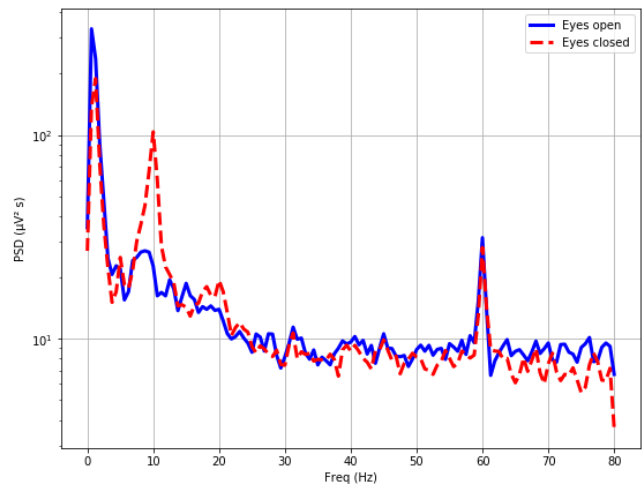


**Figure 3.** EEG PSD using Welch method for channel Iz with O and C.

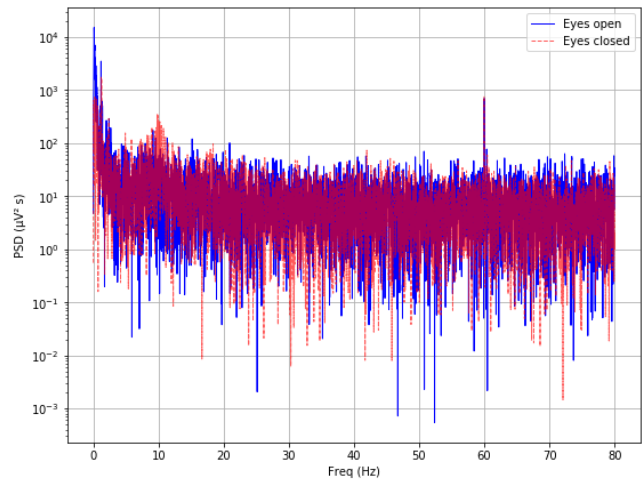


**Figure 4.** EEG PSD using Periodogram method for channel Iz with O and C.

On Figure 5 below we can see when there are SSD between C and O for the whole spectrum. The P-value on each channel colored in green when there was SSD ( $P < 0.05$ ) and in color red when there were not ( $P > 0.05$ ). As we can see in this Figure, for the Welch method we obtain that most SSD are in the mid-top part of the plane, which corresponds to the frontal lobe, except for the Iz channel, situated at the very bottom of the figures or occipital lobe. On the other hand, we can see that for the Periodogram method presents a similar polarization. We remark that these differences are evaluated over the range 0 - 80 Hz, hence small local variations in the PSD will not necessarily lead to SSD.

The average values of the PSD for the different waves in all channels using Welch are shown in Figure 6. The statistical tests showed that with always  $P - value < 0.001$  the density in delta waves is greater in O with respect to C ( $315 \pm 231 \mu V^2 s$  vs  $177 \pm 61 \mu V^2 s$ ), the density in theta waves is greater in O with respect to C ( $62 \pm 47 \mu V^2 s$  vs  $38 \pm 12 \mu V^2 s$ ), the density in alpha waves is greater in C with respect to O ( $30 \pm 8 \mu V^2 s$  vs  $21 \pm 8 \mu V^2 s$ ) and the density in beta waves is greater in C with respect to O ( $9 \pm 3 \mu V^2 s$  vs  $7 \pm 2 \mu V^2 s$ ).

The ANLD shown is in Appendix D in Figure 20 for all the frequencies and at the alpha peak wave, 10Hz, via Welch between C and O. We can see that there is great variance among the channels. The channels that have a greatest difference in the whole spectrum are Af8, Af4, F6 and Fp1, and at alpha peak are instead Pz, Poz, Cpz and Fc2. The mean value, taken over all channels, of the logarithmic difference at the alpha peak is  $95 \pm 40$ , meaning that, by far, the alpha waves are more intense in C than in O.

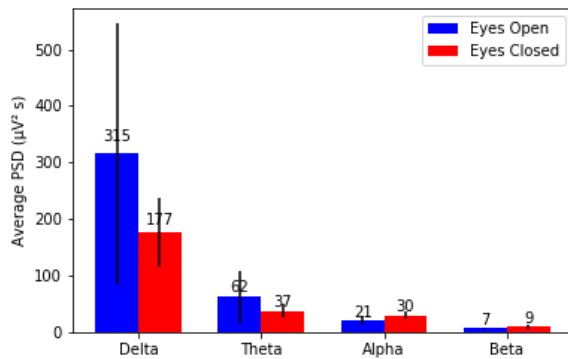


**Figure 6.** Average values standard deviation bars of the Welch PSD for the different waves in all channels for the main brain waves

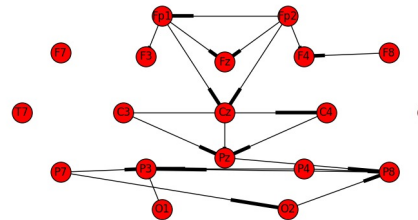
This results partially conflict with the results of [10]. Like in this analysis, C leads to a greater PSD than O in alpha and beta waves. However, in their work also there is a reduction in PSD in delta and theta waves, just the opposite than in our analysis. It is important to remark that in our analysis we

work with  $N = 1$ , and it would be interesting to determine in further work if this conflict is caused by the limitations of our dataset or sample size.

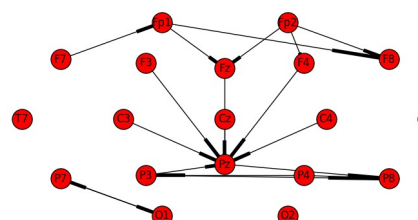
## 2.2 Connectivity graph

In order to estimate functional brain connectivity among the 64 channels, we used both MVAR estimators. Full results can be found in Appendix B in Figure 16 while here we show a topographical representation for 19 uniformly chosen channels.

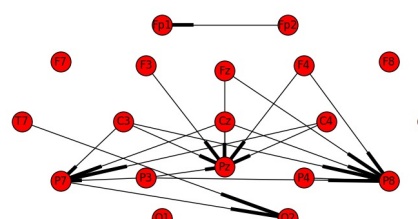
Topographical representation of the network (eyes open) based on PDC with density d=5% (top view, nose up)



Topographical representation of the network (eyes closed) based on PDC with density d=5 (top view, nose up)



Topographical representation of the network (eyes open) based on DFT with density d=5% (top view, nose up)



Topographical representation of the network (eyes closed) based on DFT with density d=5% (top view, nose up)

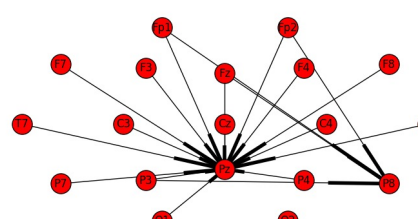


**Figure 7.** Topographical representation of the network under different conditions built with DTF and PDC estimators

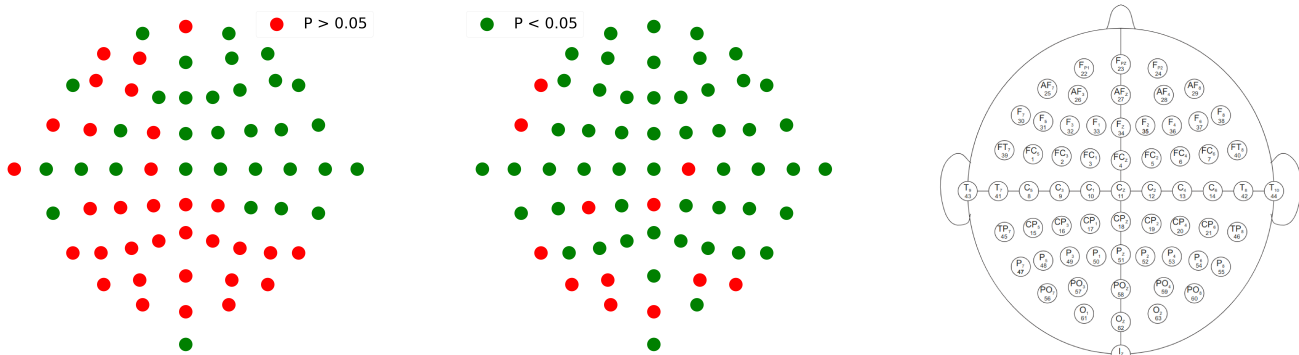


**Figure 5.** P-value of Wilcoxon test showing SSD ( $P < 0.05$  in green and  $P > 0.05$  in red) differences on O and C using on the left Welch and in the center Periodogram PSD. In the right subfigure taken from [5] we find the location of each channel

As it was shown before, frequency  $10\text{Hz}$  shows the most significant difference between two datasets C and O (Graphical results for a delta frequency can be found in Appendix B ??). We have fixed the threshold in a way to guarantee density around 20% for all estimators. The resulted representations can be found on the Figure 7.

As we can see on the Figure 7 with PDC estimator (two top subfigures), when the subject is in C we can observe that approximately 50% of the connection remains the same and the rest is changing. It seems like the network is becoming more concentrated around parietal central channels.

Since DTF is taking into account also indirect influence, it is reasonable to observe more connections in the network on the Figure 7 for DTF (two bottom subfigures). Here we see even more obvious concentration around central parietal channels than before. In fact, we can confirm this observation with PSD of the Fz channel (Figure 15 from the Appendix A) where there is an SSD between signals on  $10\text{ Hz}$  frequency.

### 2.3 Graph theory indices

We performed analysis of graph indices in two possible perspectives. Firstly, we considered the same networks as in subsection 2.2 (i.e. networks that have the same density equal to 20%). We computed the global and local indices and analyzed the results. Secondly, we studied the behavior of global graph indices as a function of the network density.

#### 2.3.1 Graph theory indices study for a fixed density

The global indices are shown in Table 1. We can observe that the average shortest path lengths are similar when using DFT networks on states C and O. On the other hand, with PDC it is much lower in O with respect to C (0.41 vs 1.61). Moreover, the average clustering coefficient is similar in O and C (in each PSD technique).

The node degree distribution is represented in Figure 8. We can see that PDC and DFT lead to different density distributions. DFT is much more skewed than PDC, although their median<sup>3</sup> node degrees are similar ( $18 \pm 20$  vs  $22 \pm 16$ ). Some

of the nodes that repeatedly show high degree are  $Poz$ ,  $Pz$ ,  $Oz$  and  $Iz$ . The first two ones already stood out in the Spectral Analysis of the alpha peak. The Tables 4 to 15 present the results for all the local indices.

For both DFT and PDC there are not SSD between C and O for the total degree distribution ( $P$ -value  $> 0.51$  and  $P$ -value  $> 0.81$  respectively).

However, there is a big difference in the magnitude of in degree and out degree indices for DFT, the medians are  $2 \pm 20$  and  $12 \pm 3$ , but not for PDC,  $11 \pm 11$  and  $11 \pm 14$ .

Graph	Avg. clustering coef.	Ave. path length
PDC C	0.31	1.61
PDC O	0.32	0.41
DFT C	0.4	1.04
DFT O	0.38	1.04

**Table 1.** Global graph indices

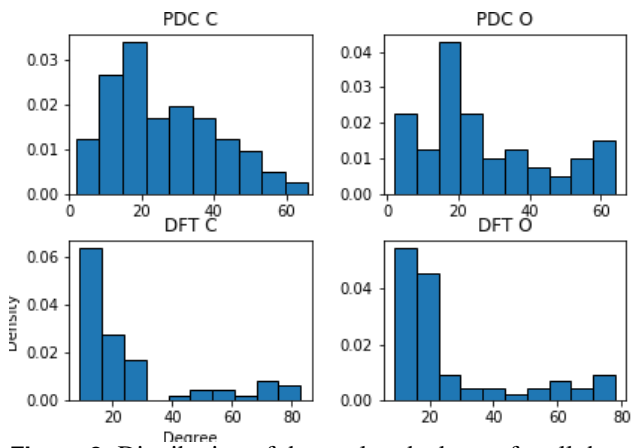


**Figure 8.** Distribution of the total node degree for all the networks.

Now comparing the C and O conditions we found that for PDC, with  $P$ -value  $< 0.001$  the out degree index is significantly lower for O than for C (medians  $13 \pm 5$  vs  $1 \pm 19$ ). This difference means that most of the nodes, in this case,

<sup>3</sup>We chose the median instead of the mean because the distributions are skewed

have only a few out edges, while only a few nodes have many out edges.

### 2.3.2 Behaviour of global graph indices with respect to network density

In order to study the behavior of global graph indices, we fixed density on 9 possible values: 1%, 5%, 10%, 15%, 20%, 25%, 30%, 35%, 40% and performed an analysis on both datasets and for both estimators.

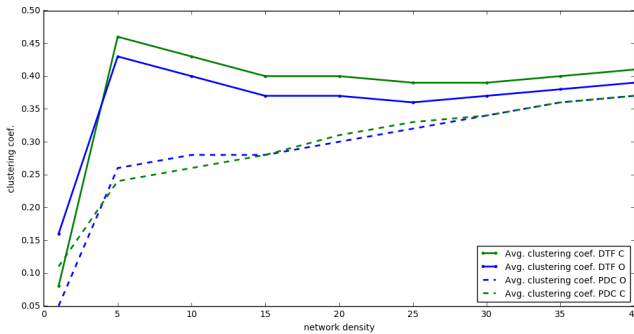


**Figure 9.** Average clustering coefficient for different densities

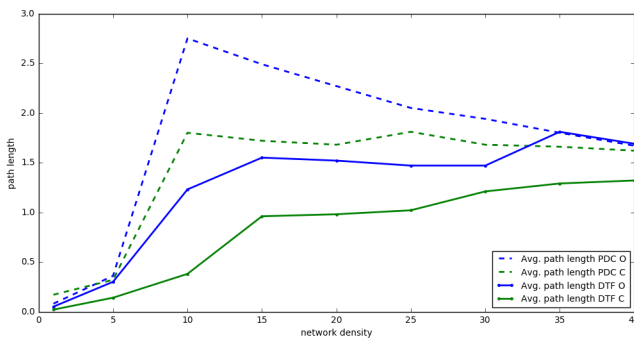


**Figure 10.** Average path length for different densities

On the Figure 9 we can observe that networks which were built with DTF estimator tend to have much higher average clustering coefficient and it seems like a natural result if we consider that DTF is taking into account indirect connections as well. An interesting result for this network is that increasing density does not always lead to increasing clustering coefficient (on the interval from 5% to 15%). This effect takes place probably because the "neighborhood" of a single node is becoming bigger while interconnections inside "the neighborhood" are increasing more slowly and hence average clustering coefficient is getting smaller.

PDC based networks tend to have increasing clustering coefficient with increasing density. This probably means that with increasing density we get more interconnections inside a node's neighborhood rather than connections between different regions. This fact is again emphasizing difference between PDC and DTF estimators which leads to a different networks typologies

Also, we can notice that in case of DTF based networks on closed eyes dataset, the average clustering coefficient is always slightly higher. We actually observed the same behavior in point 2.2.

On the Figure 10 we see that it takes some time for all networks to reach the longest average path. It means that before this point we did not have a fully connected network and we should start our analysis from 10% density (or 15% in case of DTF).

With Figure 10 we observe the same pattern as before: PDC based networks tend to show less connectivity while between two PDS (or two DTF networks) the most connected is the one that was built based on the eyes-closed dataset.

Also, on DTF based network we can observe, that the average path length is going up with increasing density and this is strictly related to the behavior that we observed in the Figure 9. When density is increasing new edges are appearing in a way that increasing number of connected pairs of nodes rather than shorten paths between already connected nodes. We believe that this behavior can be seen also in Figure 7: PDC based network seems much more interconnected, with communities inside while DFT network has an absolutely different structure.

### 2.3.3 3-nodes motifs analysis

All possible 3-nodes motifs are represented in the Figure 11.

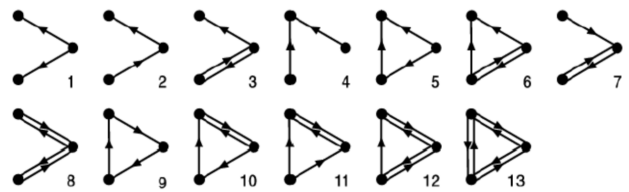


**Figure 11.** All possible 3-nodes motifs

The results on the described network are reported in the Table 2 (motifs IDs are corresponding to the Figure 11). As we can see, most of the motifs are represented in both of the networks and now we can test if any of them are over-represented, or appear to be anti-motifs.

After performing 100 simulations with random networks, we concluded, that with at least 97% probability motifs in the Table 3 are over-represented

For anti-motifs search we have fixed a threshold equal to 0.5 which means that a motif counts as anti-motif only if  $0.5 * f_{\text{random}}(G_k) > f_{\text{original}}(G_k)$ . In this setting, we did not find any anti-motifs in both networks.

Besides the mandatory task, we also were curious to determine the appearance of the particular motif S4:2  $\leftarrow$  1  $\rightarrow$  3 and then create a topographical representation of the networks considering only the connections involved in this configuration.

This motif appeared 44 times in the original O network and 63 times in the C network. It was an interesting result that both reconstructed networks (Figure 12) had almost the same density as the original one.

Motif	Freq. O	Freq. C
S1: [(2 → 1), (2 → 3)]	19	9
S2: [(2 → 1), (3 → 2)]	56	27
S3: [(2 → 1), (2 ↔ 3)]	2	5
S4: [(2 → 1), (3 → 1)]	44	63
S5: [(3 → 1), (2 → 1), (2 → 3)]	18	19
S6: [(3 → 1), (2 → 1), (2 ↔ 3)]	3	6
S7: [(1 → 2), (2 ↔ 3)]	17	21
S8: [(1 ↔ 2), (2 ↔ 3)]	0	0
S9: [(1 → 2), (2 → 3), (3 → 1)]	0	0
S10: [(1 ↔ 2), (2 → 3), (3 → 1)]	2	3
S11: [(1 ↔ 2), (3 → 2), (3 → 1)]	7	6
S12: [(3 → 1), (1 ↔ 2), (2 ↔ 3)]	4	6
S13: [(1 ↔ 2), (2 ↔ 3), (1 ↔ 3)]	1	2

**Table 2.** Motifs frequencies

Motif ID	Over-rep. in O	Over-rep. in C
S2	yes	no
S5	yes	no
S6	yes	yes
S11	yes	yes
S12	yes	yes
S13	yes	yes

**Table 3.** Over-represented 3-nodes motifs

### 2.3.4 4-nodes motifs

Due to a wide range of all possible 4 nodes directed graphs, we will list here results only for over-represented motifs. We performed analysis regarding anti-motifs as well, but there was not any 4-nodes motif that would have at least twice bigger frequency in random networks compared to the original one.

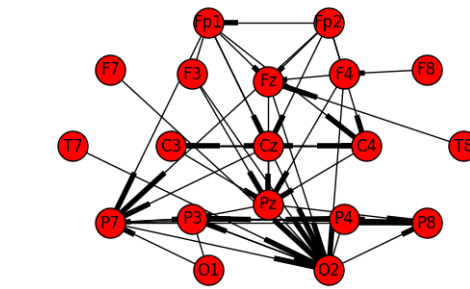
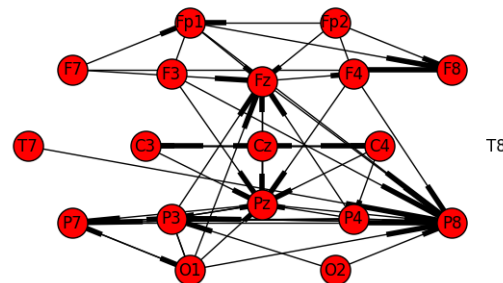
Since the table is quite big, it can be found in Appendix D in Tables 17 and 18.

The main result is that 43 4-nodes motifs are over-represented in O and 45 motifs are over-represented in C while only 17 of the motifs are over-represented in both datasets. This confirms that 2 networks have quite a different structure of connections between nodes.

### 2.4 Community detection

For DFT networks we found 4 communities in both states C and O while for PDC we found 3. The list of channels on each community can be found on Tables 19 to 22 on the Appendix D. We also represented the topographies in Figure 13. In this Figure, the size of the nodes are proportional to their respective total degrees and each color represent one community ID and their relative positions are the physical ones. The labels of the nodes are omitted to allow better visualization, but they can be identified using Figure 5.

A visual analysis for PDC clearly shows a clustering of nodes in the occipital lobe that is more exacerbated in the status O. However, this phenomena does not appear with DFT. A plausible explanation is that this is happening because PDC considers only direct interactions, and those interactions are

**Figure 12.** The network for the motif analysis

more likely in a physically near region, while DFT considers also indirect interactions.

### 3. Conclusion

After analyzing the electroencephalography signals from a single subject with eyes-open and eyes-closed baseline conditions in various perspectives we found significant differences that may be taken into account while working with these baselines. First of all, the spectral analysis showed that a frequency of 10 Hz explains the most significant difference between the two baselines, providing a higher power spectral density in the eyes-closed condition.

Moreover, different MVAR estimators to build the network of EEG signals can lead to very different graphs, and an estimator that involves only direct interactions seem to generate a topology where communities are physically close in the brain.

Also, we highlighted specific motifs which could be used as identifiers of each of the baselines. For example the motif  $A \rightarrow B \rightarrow C \rightarrow D$  is highly over-represented in O while motif  $A \leftrightarrow B, A \rightarrow C \rightarrow B, D \rightarrow C$  is over-represented for C.

Finally, in order to be more determined about archived results in further research we would suggest to examine data from several subjects and thus we would be able to determine statistical significance of all the differences listed above.

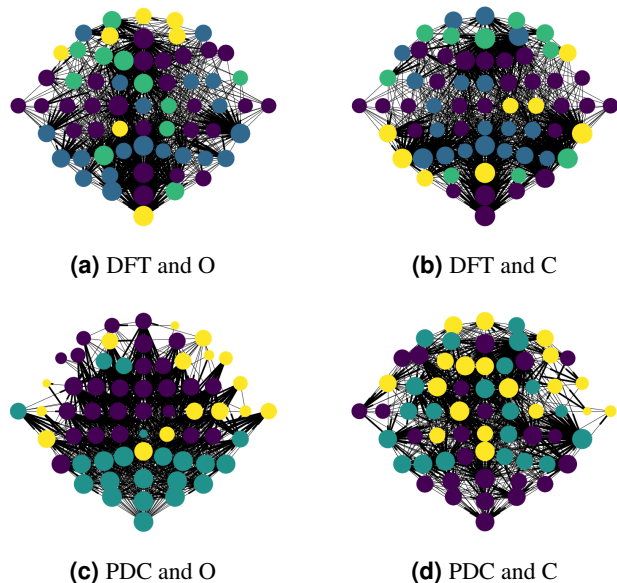


**Figure 13.** Topography of the communities using Louvain

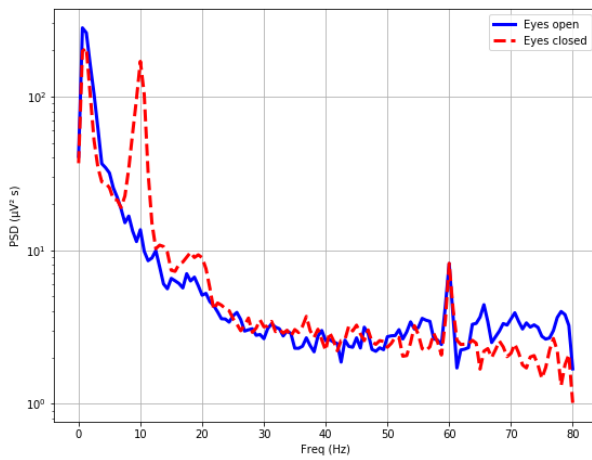
## References

- [1] Millet, David (2002). "The Origins of EEG". International Society for the History of the Neurosciences (ISHN)
- [2] Karson CN, Coppola R, Daniel DG, Weinberger DR. Computerized EEG in schizophrenia. *Schizophr Bull.* 1988;14:193–197
- [3] Thatchera RW, Northa D, Biver C. EEG and intelligence: Relations between EEG coherence, EEG phase delay and power. *Clin Neurophysiol.* 2005;116:2129–2141
- [4] Alexandre Gramfort, Partial Directed Coherence and Direct Transfer Function using MVAR processes, Github repository: <https://gist.github.com/agramfort/9875439>
- [5] Goldberger AL, Amaral LAN, Glass L, Hausdorff JM, Ivanov PCh, Mark RG, Mietus JE, Moody GB, Peng C-K, Stanley HE. PhysioBank, PhysioToolkit, and PhysioNet: Components of a New Research Resource for Complex Physiologic Signals. *Circulation* 101(23):e215-e220 [Circulation Electronic Pages; <http://circ.ahajournals.org/cgi/content/full/101/23/e215>]; 2000 (June 13). <https://physionet.org/physiobank/database/eegmmidb/>
- [6] Scipy signal processing Version 1.0.0 <https://docs.scipy.org/doc/scipy/reference/signal.html>
- [7] Lowry, Richard. "Concepts and Applications of Inferential Statistics" <http://vassarstats.net/textbook/ch12a.html>
- [8] Emmons S, Kobourov S, Gallant M, Börner K. Analysis of Network Clustering Algorithms and Cluster Quality Metrics at Scale. Dovrolis C, ed. *PLoS ONE*. 2016;11(7):e0159161. doi:10.1371/journal.pone.0159161.
- [9] Vincent Traag, Louvain igraph, (2017), GitHub repository, <https://github.com/vtraag/louvain-igraph>
- [10] Barry R. J., Clarke A. R., Johnstone S. J., Magee C. A., Rushby J. A. (2007). EEG differences between eyes-closed and eyes-open resting conditions. *Clin. Neurophysiol.* 118 2765–2773. 10.1016/j.clinph.2007.07.028
- [11] Milo, R. (2002). Network Motifs: Simple Building Blocks of Complex Networks. *Science*, 298(5594), pp.824-827.

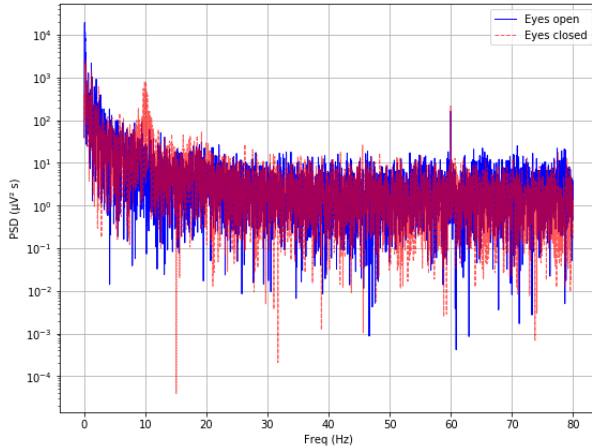
## 4. Appendix

### 4.1 Appendix A

The following Figures are the PSD of two different channels obtained with Welch and Periodogram methods:

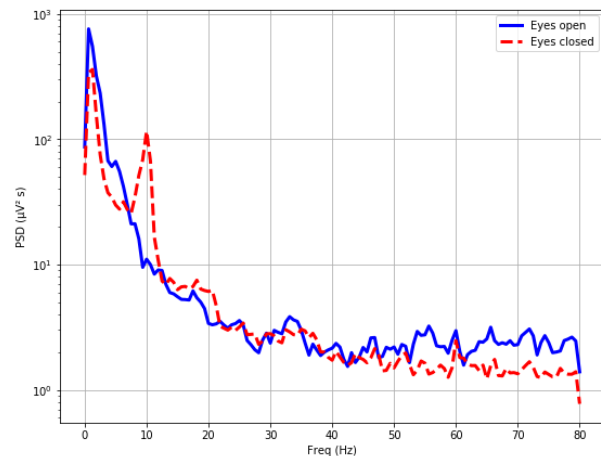


(a) Welch method

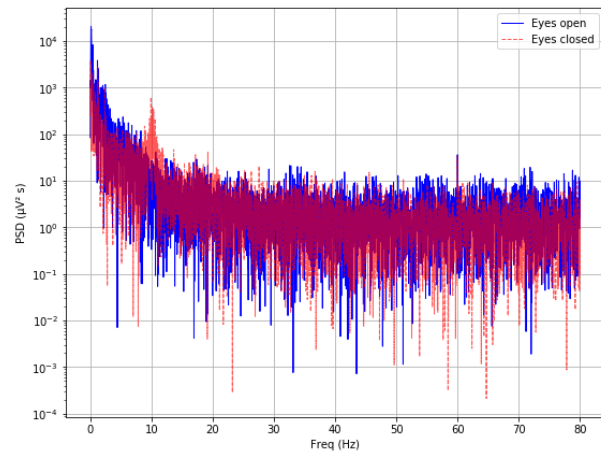


(b) Periodogram method

Figure 14. EEG PDS for channel Pz with O and C



(a) Welch method



(b) Periodogram method

Figure 15. EEG PDS for channel Fz with O and C

## 4.2 Appendix B

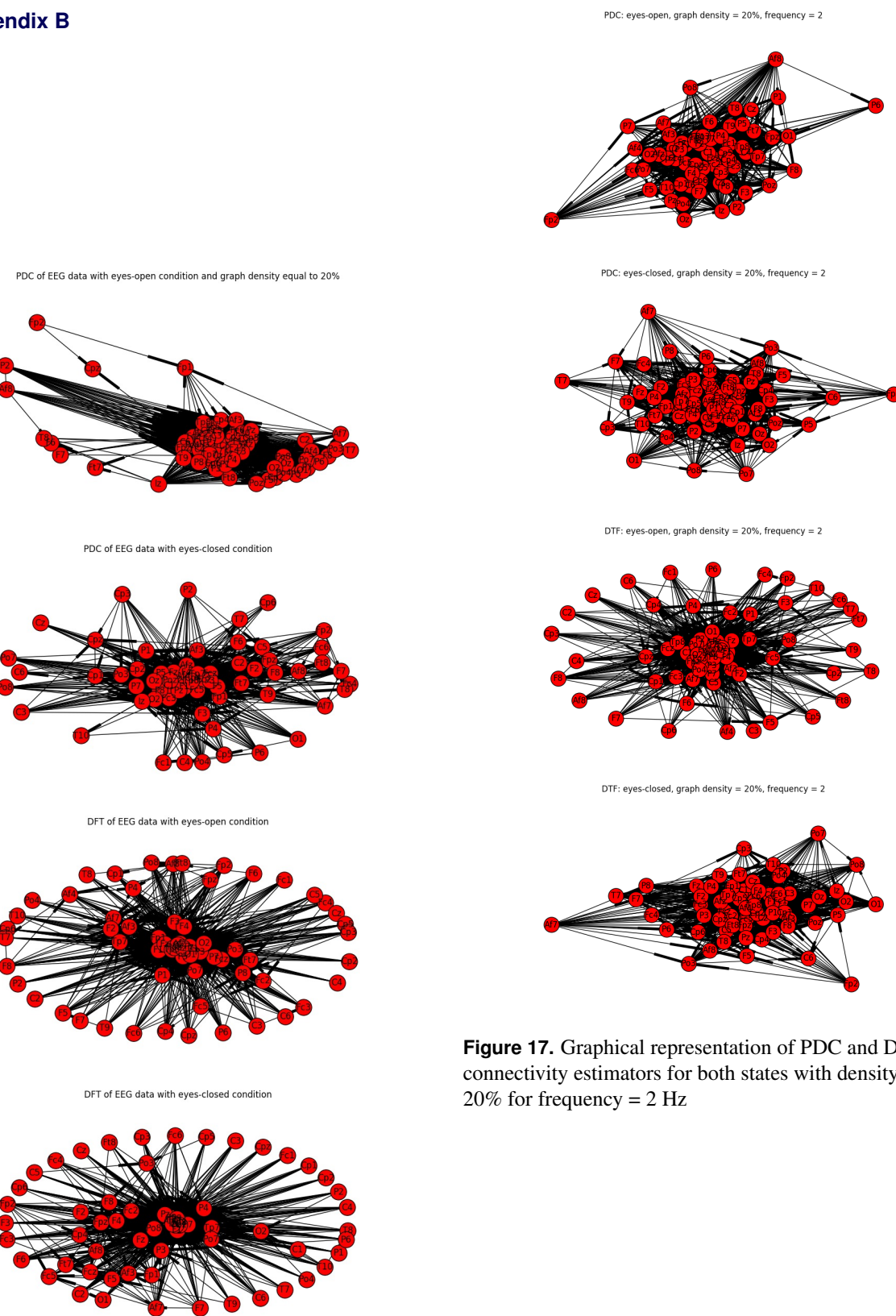


**Figure 17.** Graphical representation of PDC and DTF connectivity estimators for both states with density equal to 20% for frequency = 2 Hz

**Figure 16.** Graphical representation of PDC and DTF connectivity estimators for both states with density equal to 20%

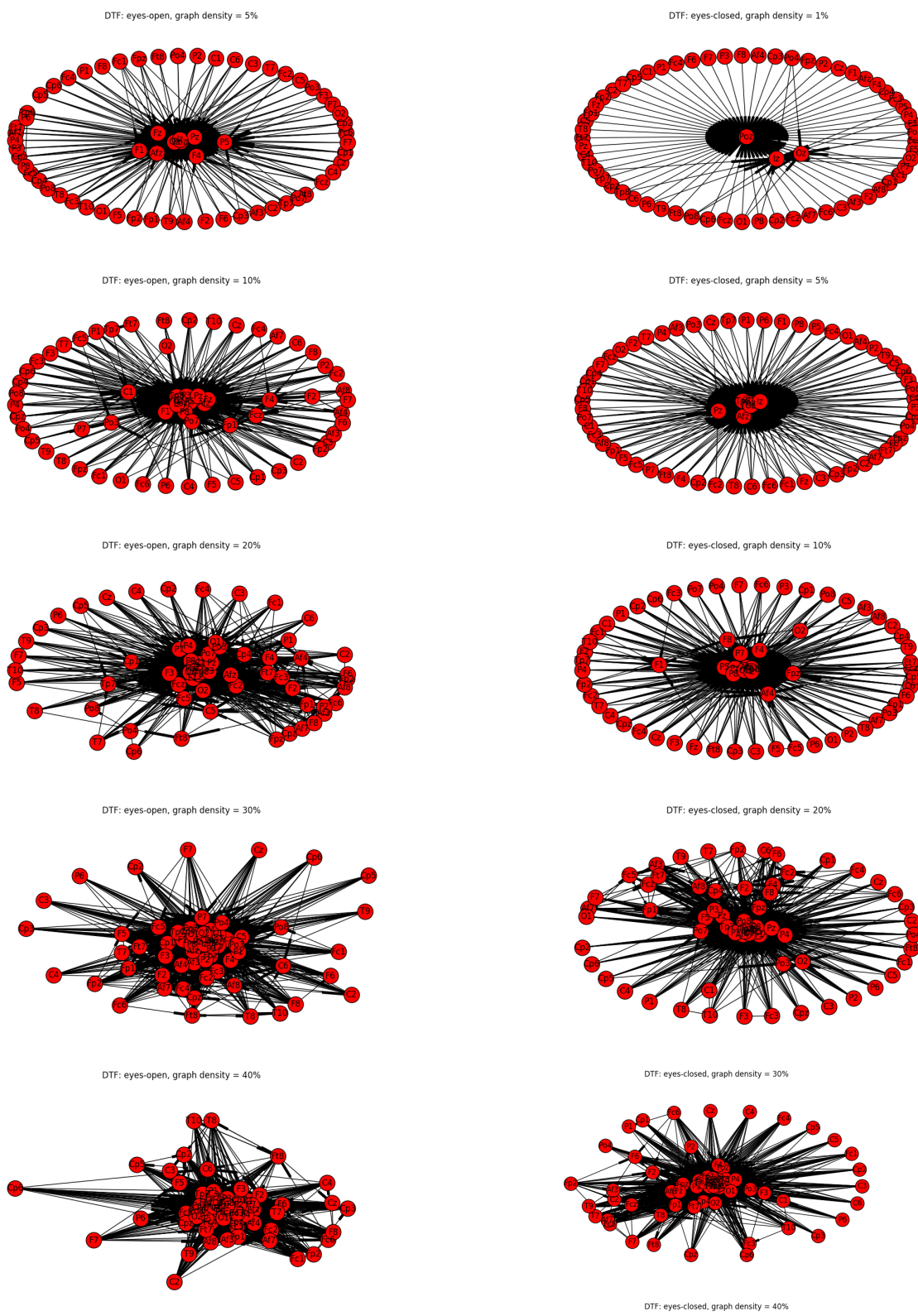


**Figure 18.** Graphical representation of DTF connectivity for O and different densities

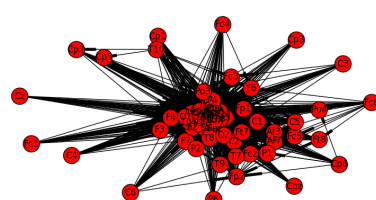


**Figure 19.** Graphical representation of DTF connectivity for C and different densities

### 4.3 Appendix C

Below are the tables showing the top ten highest degrees, in degree and out degree channels for all the networks:

Channel	Degree
Afz	83
Iz	78
Tp8	77
P5	71
Oz	71
Poz	70
P8	69
Af4	66
Pz	59
P7	57

**Table 4.** Top out degree of local graph channels with DFT method and C

Channel	Degree
Afz	78
Iz	75
Poz	73
Oz	72
C1	66
Pz	66
Fz	62
F1	61
O1	58
P3	57

**Table 7.** Top out degree of local graph channels with DFT method and O

Channel	In degree
Afz	63
Tp8	63
Oz	63
Poz	63
Iz	63
P5	60
P8	58
Pz	48
Af4	47
P7	45

**Table 5.** Top in degree of local graph channels with DFT method and C

Channel	In degree
Poz	63
Afz	62
Iz	62
Oz	62
Pz	57
C1	52
F1	49
Fz	48
O1	47
P3	45

**Table 8.** Top in degree of local graph channels with DFT method and O

Channel	Out degree
Fpz	22
Fp2	21
Fp1	21
Afz	20
Af7	20
Af4	19
F8	18
Af8	18
Af3	17
Fc4	16

**Table 6.** Top total degree of local graph channels with DFT method and C

Channel	Out degree
Af4	19
Fp2	19
Af8	19
C3	18
F6	17
F8	17
Fc3	17
Fc5	17
F5	17
Fc2	17

**Table 9.** Top total degree of local graph channels with DFT method and O

Channel	Degree
Tp8	66
Af4	58
Poz	55
Afz	51
Fc2	51
Pz	50
C1	49
P3	44
F1	44
Cp4	43

**Table 10.** Top out degree of local graph channels with PDC method and C

Channel	Degree
Oz	64
O1	62
P1	61
P4	59
O2	58
Po4	58
Iz	57
P3	57
Poz	53
Po7	53

**Table 13.** Top out degree of local graph channels with PDC method and O

Channel	In degree
Tp8	57
Af4	48
Fc2	43
Poz	40
Afz	39
C1	37
F1	35
Pz	33
Cp4	31
Fcz	30

**Table 11.** Top in degree of local graph channels with PDC method and C

Channel	In degree
Fcz	28
Fc3	27
Fc2	27
Fc5	25
C1	25
Fc4	24
Fc1	23
C3	23
C6	23
Cp1	22

**Table 14.** Top in degree of local graph channels with PDC method and O

Channel	Out degree
Iz	25
Af7	25
Fp1	24
Af3	22
P2	20
O1	20
F7	20
Fpz	20
Po7	20
P6	18

**Table 12.** Top total degree of local graph channels with PDC method and C

Channel	Out degree
Iz	57
O1	53
Oz	52
Poz	49
O2	46
Po4	46
Po7	46
Po3	46
P1	45
P4	43

**Table 15.** Top total degree of local graph channels with PDC method and O

#### 4.4 Appendix D

Task	Class
1.1	mandatory
1.2	B
1.5	E
2.1	mandatory
2.2	A
2.3	A
2.5	C
2.6	B
3.1	mandatory
3.3	D
3.4	C
3.5	B
3.6	B
4.1	mandatory
4.2	C
4.4	E
5.1	mandatory
5.2	B

**Table 16.** List of completed tasks

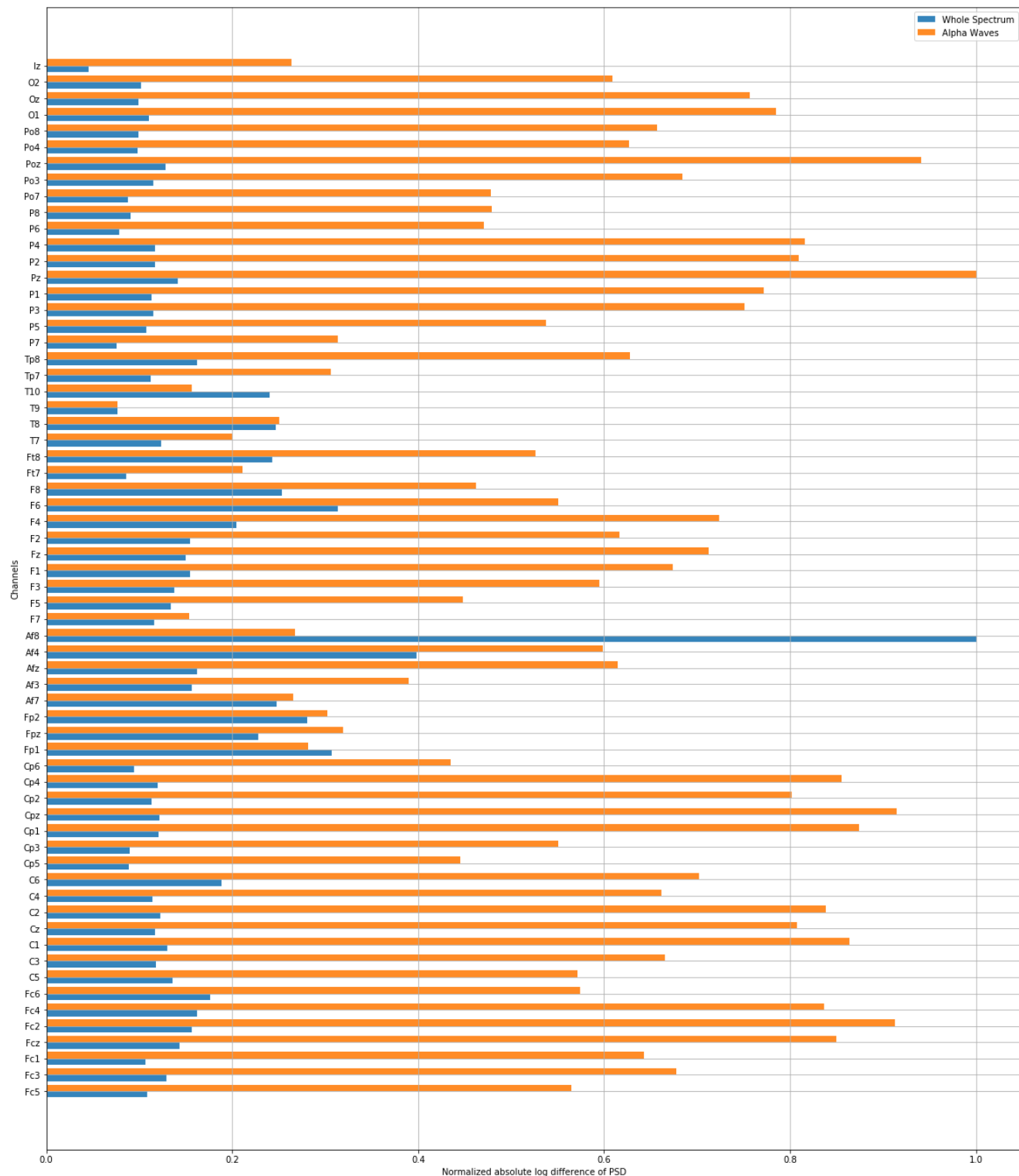


**Figure 20.** Accumulative normalized logarithmic differences between O and C of the EEG Welch PSD on each channel. In orange for only alpha waves, and in blue all waves.

	Pattern	Freq. O	Freq Q
S66	[(1; 2); (1; 3); (2; 3); (3; 4); (4; 3)]	8	not over-repr.
S88	[(1; 2); (1; 3); (2; 1); (2; 3); (3; 1); (4; 1)]	not over-repr.	6
S11	[(1; 2); (1; 3); (1; 4); (2; 3)]	15	not over-repr.
S42	[(1; 2); (1; 3); (2; 1); (2; 3); (4; 1)]	not over-repr.	6
S28	[(1; 2); (2; 1); (3; 1); (4; 2)]	not over-repr.	16
S132	[(1; 2); (1; 3); (1; 4); (2; 1); (2; 3); (4; 2); (4; 3)]	not over-repr.	2
S114	[(1; 2); (1; 3); (2; 3); (2; 4); (3; 4); (4; 3)]	4	not over-repr.
S195	[(1; 2); (1; 3); (1; 4); (2; 1); (2; 3); (2; 4); (3; 1); (3; 2); (3; 4); (4; 1)]	not over-repr.	1
S62	[(1; 2); (1; 3); (2; 3); (3; 2); (4; 1)]	19	2
S17	[(1; 2); (1; 3); (2; 3); (2; 4)]	not over-repr.	6
S93	[(1; 2); (1; 3); (2; 1); (2; 3); (4; 1); (4; 2)]	2	not over-repr.
S175	[(1; 2); (1; 3); (1; 4); (2; 3); (2; 4); (3; 2); (3; 4); (4; 2)]	1	4
S158	[(1; 2); (1; 3); (1; 4); (2; 1); (2; 3); (2; 4); (3; 1); (4; 2)]	not over-repr.	1
S123	[(1; 2); (1; 3); (1; 4); (2; 1); (2; 3); (3; 1); (4; 3)]	not over-repr.	1
S13	[(1; 2); (1; 3); (2; 1); (3; 4)]	6	10
S51	[(1; 2); (1; 3); (2; 1); (3; 2); (4; 2)]	not over-repr.	6
S63	[(1; 2); (1; 3); (2; 3); (3; 2); (4; 2)]	not over-repr.	27
S67	[(1; 2); (1; 3); (2; 3); (4; 2); (4; 3)]	4	11
S159	[(1; 2); (1; 3); (1; 4); (2; 1); (2; 3); (2; 4); (3; 1); (4; 3)]	not over-repr.	1
S7	[(1; 2); (2; 3); (4; 2)]	62	not over-repr.
S108	[(1; 2); (1; 3); (2; 1); (3; 2); (4; 1); (4; 2)]	not over-repr.	3
S22	[(1; 2); (1; 3); (2; 4); (3; 4)]	14	not over-repr.
S8	[(1; 2); (2; 3); (4; 3)]	83	not over-repr.
S43	[(1; 2); (1; 3); (2; 1); (2; 3); (4; 3)]	9	20
S193	[(1; 2); (1; 3); (1; 4); (2; 1); (2; 3); (3; 2); (3; 4); (4; 2); (4; 3)]	2	not over-repr.
S9	[(1; 2); (3; 2); (4; 2)]	not over-repr.	73
S144	[(1; 2); (1; 3); (2; 1); (2; 3); (3; 1); (4; 1); (4; 2)]	2	not over-repr.
S135	[(1; 2); (1; 3); (1; 4); (2; 1); (3; 2); (3; 4); (4; 3)]	not over-repr.	1
S83	[(1; 2); (1; 3); (1; 4); (2; 3); (2; 4); (3; 2)]	2	2
S2	[(1; 2); (1; 3); (2; 4)]	30	not over-repr.
S185	[(1; 2); (1; 3); (1; 4); (2; 1); (2; 3); (2; 4); (3; 1); (3; 4); (4; 1)]	1	2
S84	[(1; 2); (1; 3); (1; 4); (2; 3); (2; 4); (3; 4)]	2	not over-repr.
S1	[(1; 2); (1; 3); (1; 4)]	7	not over-repr.
S24	[(1; 2); (1; 3); (2; 4); (4; 2)]	20	not over-repr.
S146	[(1; 2); (1; 3); (2; 1); (2; 3); (3; 1); (4; 2); (4; 3)]	1	2
S33	[(1; 2); (1; 3); (1; 4); (2; 1); (2; 3)]	2	not over-repr.
S19	[(1; 2); (1; 3); (2; 3); (4; 1)]	16	not over-repr.

Table 17. Over-represented 4-nodes motifs for O and C

	Pattern	Freq. O	Freq Q
S50	[(1; 2); (1; 3); (2; 1); (3; 2); (4; 1)]	9	not over-repr.
S139	[(1; 2); (1; 3); (1; 4); (2; 3); (2; 4); (3; 4); (4; 3)]	2	not over-repr.
S94	[(1; 2); (1; 3); (2; 1); (2; 3); (4; 1); (4; 3)]	not over-repr.	4
S197	[(1; 2); (1; 3); (1; 4); (2; 1); (2; 3); (2; 4); (3; 1); (3; 2); (4; 1); (4; 3)]	not over-repr.	1
S176	[(1; 2); (1; 3); (2; 1); (2; 3); (3; 1); (3; 2); (4; 1); (4; 2)]	2	1
S186	[(1; 2); (1; 3); (1; 4); (2; 1); (2; 3); (2; 4); (3; 1); (3; 4); (4; 2)]	not over-repr.	1
S155	[(1; 2); (1; 3); (1; 4); (2; 1); (2; 3); (2; 4); (3; 1); (3; 2)]	not over-repr.	1
S41	[(1; 2); (1; 3); (2; 1); (2; 3); (3; 4)]	9	7
S141	[(1; 2); (1; 3); (2; 1); (2; 3); (3; 1); (3; 4); (4; 1)]	not over-repr.	1
S187	[(1; 2); (1; 3); (1; 4); (2; 1); (2; 3); (2; 4); (3; 1); (3; 4); (4; 3)]	not over-repr.	1
S138	[(1; 2); (1; 3); (1; 4); (2; 3); (2; 4); (3; 2); (4; 3)]	not over-repr.	1
S119	[(1; 2); (1; 3); (1; 4); (2; 1); (2; 3); (3; 1); (3; 2)]	1	1
S169	[(1; 2); (1; 3); (1; 4); (2; 1); (2; 3); (3; 2); (3; 4); (4; 2)]	1	not over-repr.
S21	[(1; 2); (1; 3); (2; 3); (4; 3)]	32	not over-repr.
S76	[(1; 2); (1; 3); (1; 4); (2; 1); (2; 3); (4; 3)]	not over-repr.	4
S52	[(1; 2); (1; 3); (2; 1); (3; 2); (4; 3)]	not over-repr.	7
S40	[(1; 2); (1; 3); (1; 4); (2; 3); (4; 3)]	4	not over-repr.
S145	[(1; 2); (1; 3); (2; 1); (2; 3); (3; 1); (4; 1); (4; 3)]	3	5
S90	[(1; 2); (1; 3); (2; 1); (2; 3); (3; 1); (4; 3)]	6	18
S5	[(1; 2); (2; 1); (3; 4)]	69	98
S18	[(1; 2); (1; 3); (2; 3); (3; 4)]	21	not over-repr.
S30	[(1; 2); (2; 1); (3; 4); (4; 3)]	10	12
S136	[(1; 2); (1; 3); (1; 4); (2; 3); (2; 4); (3; 2); (3; 4)]	not over-repr.	2
S6	[(1; 2); (2; 3); (3; 4)]	36	not over-repr.
S20	[(1; 2); (1; 3); (2; 3); (4; 2)]	29	not over-repr.
S38	[(1; 2); (1; 3); (1; 4); (2; 3); (3; 2)]	5	not over-repr.
S59	[(1; 2); (1; 3); (2; 3); (2; 4); (3; 4)]	9	5
S37	[(1; 2); (1; 3); (1; 4); (2; 3); (2; 4)]	4	2
S140	[(1; 2); (1; 3); (2; 1); (2; 3); (3; 1); (3; 2); (4; 1)]	not over-repr.	1
S89	[(1; 2); (1; 3); (2; 1); (2; 3); (3; 1); (4; 2)]	11	9
S182	[(1; 2); (1; 3); (1; 4); (2; 1); (2; 3); (2; 4); (3; 1); (3; 2); (3; 4)]	1	1
S92	[(1; 2); (1; 3); (2; 1); (2; 3); (3; 4); (4; 3)]	not over-repr.	6

**Table 18.** Over-represented 4-nodes motifs for O and C

Community ID	Elements	Channels
0	26	Fc3 Fc2 C5 C3 C1 C4 Cp5 Cp3 Cpz Cp4 Cp6 Afz Fz F2 F4 F6 F8 Ft7 T7 T8 T9 T10 Poz Po4 Po8 Oz
1	20	Fc1 Fc4 Fc6 Cz C6 Af7 Af8 Tp7 Tp8 P7 P5 P1 Pz P2 P4 P6 P8 Po7 Po3 O1
2	11	Fc5 Fcz C2 Cp2 Fp1 F5 F3 F1 Ft8 P3 O2
3	7	Cp1 Fpz Fp2 Af3 Af4 F7 Iz

**Table 19.** Communities found using Louvain for DFT with O

Community ID	Elements	Channels
0	27	Fc3 Fc2 Fc4 Fc6 C5 C1 Cz C6 Cp5 Cp1 Cp6 F5 F3 F1 Fz F2 F4 Ft8 T7 T8 T9 T10 Po8 O1 Oz O2 Iz
1	19	Fc5 Fc1 Fcz C3 Cp3 Cpz Cp2 Cp4 Fp1 Fpz Af4 F7 P5 P3 P1 Pz P2 P4 P6
2	10	Fp2 Af7 Af3 Afz Af8 F6 Ft7 P8 Po3 Po4
3	8	C2 C4 F8 Tp7 Tp8 P7 Po7 Poz

**Table 20.** Communities found using Louvain for DFT with C

Community ID	Elements	Channels
0	27	Fc5 Fc3 Fc1 Fcz Fc2 Fc4 Fc6 C5 C3 C1 Cz C2 Cp5 Cp3 Cp1 Cp4 Cp6 Fp1 Fpz Af7 Afz Af4 F7 F5 Fz F2 P7
1	21	Cpz F3 F1 T9 Tp8 P5 P3 P1 P2 P4 P6 P8 Po7 Po3 Poz Po4 Po8 O1 Oz O2 Iz
2	16	C4 C6 Cp2 Fp2 Af3 Af8 F4 F6 Ft7 Fz T7 T8 T10 Tp7 Pz

**Table 21.** Communities found using Louvain for PDC with O

Community ID	Elements	Channels
0	24	Fc1 Cz Cp5 Cp1 Cp4 Cp6 Afz F7 F5 F4 F8 T7 T9 P1 P8 Po7 Po3 Poz Po4 Po8 O1 Oz O2 Iz
1	21	Fc5 Fcz Fc4 C5 C3 C2 C6 Cp2 Fp2 Af7 Af3 Af4 F2 Tp7 Tp8 P7 P5 P3 P2 P4 P6
2	19	Fc3 Fc2 Fc6 C1 C4 Cp3 Cpz Fp1 Fpz Af8 F3 F1 Fz F6 Ft7 Ft8 T8 T10 Pz

**Table 22.** Communities found using Louvain for PDC with C